Effects of MWNT Nanofillers on Structures and Properties of PVA Electrospun Nanofibers

Minoo Naebe[1], Tong Lin[1*], Wendy Tian[2], Liming Dai[3] and Xungai Wang[1]

1. Centre for Material and Fibre Innovation, Deakin University, Geelong, VIC 3217, Australia
2. Molecular and Health Technologies, Commonwealth Scientific and Industrial Research Organisation, Clayton, VIC 3169, Australia
3. Department of Chemical and Materials Engineering, The University of Dayton, Dayton, OH 45469, USA

Abstract: In this study, we have electrospun poly(vinyl alcohol)(PVA) nanofibers and PVA composite nanofibers containing multiwall carbon nanotubes (MWNTs) (4.5wt%), and examined the effect of the carbon nanotubes and the PVA morphology change induced by post-spinning treatments on the tensile properties, surface hydrophilicity and thermal stability of the nanofibers. Through differential scanning calorimetry (DSC) and wide angle X-ray diffraction (WAXD) characterisations, we have observed that the presence of the carbon nanotubes nucleated crystallization of PVA in the MWNTs/PVA composite nanofibers, and hence considerably improved the fiber tensile strength. Also, the presence of carbon nanotubes in PVA reduced the fiber diameter and the surface hydrophilicity of the nanofiber mat. The MWNTs/PVA composite nanofibers and the neat PVA nanofibers responded differently to post-spinning treatments, such as soaking in methanol and crosslinking with Glutaric Dialdehyde, with the purpose of increasing PVA crystallinity and establishing crosslinked

* Corresponding author, Phone: +61 (03) 5227 1245; Fax: +61 (03) 5227 2539, email: tong.lin@deakin.edu.au

PVA network, respectively. The presence of carbon nanotubes reduced the PVA crystallization rate during the methanol treatment, but prevented the decrease of crystallinity induced by the crosslinking reaction. In comparison with the crosslinking reaction, the methanol treatment resulted in better improvement in the fiber tensile strength and less reduction in the tensile strain. In addition, the presence of carbon nanotubes reduced the onset decomposition temperature of the composite nanofibers, but stabilized the thermal degradation for the post-spinning treated nanofibers. The MWNTs/PVA composite nanofibers treated by both methanol and crosslinking reaction gave the largest improvement in the fiber tensile strength, water contact angle and thermal stability.

Keywords: Electrospun nanofibers, carbon nanotubes, crystallinity, crosslink, nucleation crystallization, tensile properties, surface hydrophility, thermal stability.

1. Introduction

Carbon nanotubes (CNTs) with a high aspect-ratio and low density have been shown to possess excellent mechanical, thermal, and electronic properties [1]. These characteristics make them an ideal candidate as a filler to develop potentially revolutionary composites with light weight and enhanced mechanical[2, 3], electrical[4, 5] or thermal properties[6, 7]. Polymer fibers reinforced with CNTs are of particular interest[3, 8-15]. Super-tough CNT composite fibers have been produced by spinning single-wall carbon nanotubes (SWNTs) into poly(vinyl alcohol)(PVA) solution[3, 8, 9]. The mechanical properties of the composite fibers are highly dependent on the dispersion and the microscopic orientation of carbon nanotubes in the polymer matrix, and their interfacial interactions with the polymer.

Recently, electrospinning has been used to produce ultra-fine CNT composite fibers. The electrospinning process involves stretching a polymer solution under a strong electric field to form dry or semidry fibers with diameters on the nanometer scale[16-19]. From solution to dry fiber, the fiber stretching process takes just tens of milliseconds[20]. With such a fast fiber-stretching speed and high aspect-ratio of the resultant nanofiber, an alignment of CNTs along the axis of nanofiber could be achieved when a polymer solution containing well dispersed carbon nanotubes is electrospun[14, 15, 21, 22]. The electrospun nanofibers can be collected in the form of randomly oriented non-woven mat, aligned nanofiber array and continuous nanofiber yarn, which have shown enormous potential in diverse applications.

Electrospun composite fibers of MWNTs with different polymers such as polyvinyl alcohol(PVA)[15], polyethylene oxide (PEO)[15, 23], polyacrylonitrile (PAN)[24, 25], polycarbonate (PC)[26], nylon[27], polymethyl methacrylate (PMMA)[28], and poly(vinyl acetate) (PVAc)[29] have been reported. These composite nanofibers have shown enhanced fiber mechanical properties and improved electrical conductivity also. However, systematic study on carbon nanotube-matrix interaction has been scarce in the research literature.

PVA is a semi-crystal hydrophilic polymer consisting of one hydroxyl group in each repeat unit and hence crosslinkable. The carbon nanotube/PVA composite film and fiber have received a great deal of attention because of their excellent mechanical properties[3, 8, 30, 31] and combined electrical/thermal conductivity unavailable in other composite materials. Recent researches[2, 30-38] have indicated that CNTs nucleate crystallization of PVA, and a crystalline PVA layer formed around the nanotubes accounts for the excellent mechanical properties of the composite materials.

PVA is also one of the major polymer systems being studied in the electrospinning field. The electrospin-ability of PVA is affected by electrospinning parameters[17], the PVA molecular weights[39, 40] and hydrolyzed degrees[41], solution pH values[42] and additives[43, 44]. The PVA nanofibers have been used as drug carriers for controlled release[45, 46]. Although electrospun CNTs/PVA nanofibers have been reported[23], it has not been established if the nucleation crystallization of PVA occurs within the electrospun composite CNTs/PVA fibers, and if the fast fiber stretching in electrospinning would obstruct this nucleation crystallization process.

It has been well established that the polymer morphology, the overall form of polymer structure, is an important factor in determining the material properties. The change of PVA crystallinity and the formation of crosslinked PVA network achieved by a post-spinning treatment have been found to improve fiber mechanical properties [43, 47]. It has not yet been established if the mechanical properties of a composite CNTs/PVA fiber can be improved through the change of PVA morphology induced by a post-treatment.

In this study, we used multi-wall carbon nanotubes (MWNTs)/PVA composite nanofibers as a model material to examine the effects of carbon nanotubes and the PVA morphological changes on the polymer crystallinity, tensile properties, surface hydrophility and thermal stability of the composite fibers. Possible effects of the post-spinning treatments by soaking in methanol, crosslinking with glutaric dialdehyde, or both are also discussed. This study will contribute to our understanding of the role of polymer matrix and filler-matrix interaction in improving the properties of CNTs/polymer composite fibers. In addition, the MWNTs/PVA

nanofibers may find applications in biomedical areas, as drug carriers for controlled release for instance.

2. Experimental details

2.1. Materials and measurements

PVA (average molecular weight =146,000-186,000, 96% hydrolyzed) and all other chemicals were obtained from Aldrich-Sigma and used as received. The MWNTs were provided by CSIRO and were purified by refluxing in 3N HNO_3 for 48 hours prior to use.

The electrospun nanofibers were observed under a scanning electron microscope (SEM Leica S440) and a transmission electron microscope (TEM, Model 2000 FE, Hitachi Corp). The fiber diameter was calculated based on the SEM images with the aid of a software package (Image*Pro Plus 4.5*). The mechanical properties of the nanofiber mats were measured with a universal tensile tester (Lloyd), according to ASTM D-882. Differential scanning calorimetry (DSC) was performed using DSC 821 (Mettler Toledo). A specimen of approximately 5mg was encapsulated in an aluminium pan (13mg) and measured in alternating DSC mode at an underlying heating rate of 10^{o}C/min. Before the DSC measurements, the samples were vacuum dried for 72 hrs at room temperature in the presence of phosphorus pentoxide. Wide angle X-ray diffraction (WAXD) was done on a powder diffractometer (Philips 1140/90) with a Cu radiation 1.5406Å. Fourier Transform Infrared (FTIR) spectra were recorded by a FTIR spectrophotometer (Bruker Optics), using KBr method. The water contact angles were measured using a contact angle meter (KSV CAM200 Instruments Ltd). Thermo-gravimetric analysis (TGA) was performed with a Mettler Toledo TGA/STDA851. The specimens were placed in a ceramic pan and tested in air flow at a heating rate of 10^{o}C/min.

2.2. Electrospinning of MWNTs/PVA nanofibers

PVA aqueous solution (16wt %) was prepared by dissolving PVA powder in distilled water at 90^{o}C with constant stirring for about 12 hours. A mixture of the purified MWNTs (245mg) and water (6.25ml) was ultrasonicated for about 5 hours and then mixed with the PVA solution (16wt%, 33.75ml). During the ultrasonic process, the solution was cooled in an ice/water bath to avoid solution overheating. The solution was further ultrasonicated for one hour to obtain homogeneous dispersion. The final PVA solution contained 13.5wt% PVA and 0.6wt% MWNTs. The MWNT content based on PVA is 4.5wt%.

The electrospinning setup consists of a plastic syringe with a metal syringe needle (21 Gauge), a syringe pump (KD scientific), a high voltage power supply (ES30P, Gamma High Voltage Research) and a metal roller collector. The plastic syringe, needle and the syringe pump were fixed on a movable tackle driven by a motor, forming the moveable nozzle system. In electrospinning, the MWNTs/PVA solution was placed into the syringe and charged with 20kV electrical voltage via connecting the syringe needle to the power supply. The grounded electrode was connected to the metal roller, 15cm away from the needle tip. The flow rate of the MWNTs/PVA solution was controlled at 1.0ml/hr. During the electrospinning process, the nozzle moved to-and-fro along the axis direction of the metal roller at the speed of 20cm/min, while the metal roller rotated at a constant speed of 100 rpm. This system was able to produce relatively large (20×30cm^2) and uniform nanofiber mats. The thickness of the mats was in the range 70-200 micron. The neat PVA nanofiber mat was also electrospun from 13.5wt% PVA solution under the same operating conditions.

2.3. Post-spinning treatments of the nanofibers

The as-spun PVA fibers were subjected to different post-spinning treatments as follows:

Soaking in methanol[43]: The nanofiber mat was placed in methanol for 24 hours and then dried at 50^{o}C for 24 hours.

Crosslinking with glutaric dialdehyde[47]: The nanofiber mat was placed in a glutaric dialdehyde-acetone solution (0.05wt%, pH=2-3 adjusted by HCl) for 4 hours, and then curled at 150^{o}C for 10 min.

Methanol treatment followed by crosslinking: The nanofiber mat was first treated by methanol and then crosslinked with glutaric dialdehyde, under the same conditions as above.

3. Results and discussion

3.1. Microscopy observation

Electrospinning the plain PVA solution and the PVA solution containing MWNTs both resulted in uniform nanofibers. The average diameters of the as-spun nanofibers are listed in **Table 1**. For the neat PVA nanofibers, the average fiber diameter was about 680nm. However, the presence of MWNTs resulted in much finer nanofibers, with an average diameter of 295nm (Table 1), and the fiber distribution became very narrow as well. The large reduction in fiber diameter suggests that the presence of carbon nanotubes in PVA solution affected the fiber stretching process.

The post-spinning treatments only had a marginal effect on both the average diameter and the uniformity of the nanofibers. As listed in **Table 1**, the neat PVA nanofibers treated by methanol showed a small decrease in average fiber diameter, while crosslinking reaction led to

slightly thicker fibers. For the MWNTs/PVA composite nanofibers, both methanol and crosslinking treatments led to a slight increase in average fiber diameter (**Figure 1**).

To examine nanotube dispersion in the PVA matrix, the as-spun nanofibers solidified within a resin were sliced into specimens of 100nm thick and observed under the TEM. **Figure 2** gives a view of the dispersed carbon nanotubes. It also confirmed the existence of carbon nanotubes in the nanofiber mat.

3.2 FTIR spectra

The FTIR spectra of the PVA nanofibers containing MWNTs before and after the crosslinking reaction are shown in **Figure 3**. After the crosslinking reaction, vibration peaks at around 917cm^{-1}, 1096cm^{-1} and 1144cm^{-1} were increased, which correspond to the CH_2 rocking, C-O stretching and C-O-C bending vibration, respectively. The vibration peak in the range of 1235~1340cm^{-1} was decreased, confirming the reduction of C-H wagging and CH-OH bending vibrations. Also, an increase in the absorbance of 1700 cm^{-1} is attributed to the C=O group of the aldehyde. These changes in the FTIR spectra confirmed the occurrence of crosslinked network after the nanofibers were treated with glutaric dialdehyde [48-50].

3.3. Differential Scanning Calorimetry (DSC)

Figure 4a shows the DSC profiles measured for the neat PVA nanofibers. All the nanofibers have an endothermic peak around 200-225^{o}C, corresponding to the melting of PVA (T_m). The T_m values were listed in **Table 2**. The post-treatments shifted the T_m peak. Compared with the un-treated nanofibers, methanol treatment shifted T_m to a higher temperature, while the T_m was reduced after the crosslinking reaction.

To compare the crystallinity, enthalpy (ΔH) values were calculated by numerical integration of the area under the melting peak and normalized for sample mass. The increase in crystallinity for the PVA was calculated using the enthalpy of 155J/g for a theoretical 100% crystalline PVA[33]. The neat PVA nanofibers have a relatively low crystallinity, at just about 28.8%. The crystallinity of the methanol treated PVA nanofibers increased to 37.4%, but the crosslinking reaction reduced its crystallinity slightly, due to the change of crystalline morphology induced by the crosslinker[51]. The crystallinity of the PVA nanofibers treated by both methanol and the crosslinking reaction is between those treated by the two methods separately.

It is also worth noting that the neat PVA nanofibers contain a certain amount of water as indicated by a peak in the range of 130~170^{o}C in the DSC curves, though the samples have been dried in vacuum for 72 hours before test. This peak disappeared when the sample was scanned for the second time under the same condition. A similar phenomenon was observed in the MWNTs/PVA film[38]. The post-spinning treatments also affected both the location and height of this peak, indicating that water molecules in PVA could be incorporated into the amorphous phase. The peak reduced and shifted to a lower temperature as a result of methanol treatment, confirming that the methanol treatment removed some water from the polymer because of the increased PVA crystallization. However, this peak shifted to a higher temperature after the crosslinking reaction, suggesting that the water molecules could be trapped in the crosslinked PVA network.

By contrast, all MWNTs/PVA composite nanofibers showed higher crystallinity. As listed in **Table 2**, the crystallinity of the un-treated MWNTs/PVA nanofibers is 34.3%, about 5.5%

higher than its neat PVA counterpart. The increase in the crystallinity of PVA due to the presence of carbon nanotubes indicated the occurrence of nucleation PVA crystallization in the electrospun composite nanofibers, which is similar to the case in cast CNTs/PVA film and wet-spun fibers [2, 33, 34, 36, 38]. As the electrospinning process took place very quickly, it is less likely for the PVA molecules to nucleate crystallization around the carbon nanotubes during the electrospinning process. Since the presence of carbon nanotubes in PVA solution also led to a decrease in the fiber diameter, it is possible that this nucleation crystallization or a self-assembly of PVA on nanotube surface could happen any time as long as the carbon nanotubes are dispersed in PVA solution before electrospinning.

The post-treatments also affected the T_m temperature and the crystallinity of the MWNTs/PVA composite nanofibers (**Figure 4b**). The methanol treatment shifted the T_m to a lower value, and also increased the crystallinity content (39.5%), albeit to a lesser extent. The crosslinking reaction led to a slight decrease in T_m value, but a small increase in the crystallinity, which is quite different to the case for the neat PVA nanofibers. This slight increase in the PVA crystallinity after the crosslinking reaction suggested that the presence of carbon nanotubes restricted the reduction of PVA crystallinity induced by the crosslinker. The highest crystallinity content was found in the composite nanofibers treated by both methanol and crosslinking reaction (40.1%). This result confirmed that the presence of carbon nanotubes in the PVA matrix made the PVA perform differently in the post-spinning treatments.

In addition, water was also observed in the composite nanofibers, and the post-spinning treatments affected the water peak. The methanol treatment removed almost all the water from

the composite nanofibers because no water peak was observed in the DSC curve. However, the crosslinking reaction only shifted the peak to a lower temperature.

3.3. Wide Angle X-ray Diffraction (WAXD)

The WAXD patterns of the neat PVA nanofibers show a strong (101) peak, at about 2θ=19.4^{o} [52, 53] (**Figure 5a**). The post-spinning treatment was observed to change the (101) diffraction intensity. By comparison to the un-treated nanofibers, the nanofibers treated by methanol led to stronger (101) reflection, and the occurrence of medium intensity (001) and (002) reflections at 16.0^{o} and 32.5^{o}, respectively. However, when the nanofibers were crosslinked, the (101) reflection was lowered considerably. The PVA nanofibers treated by methanol and crosslinking reaction showed a slight reduction in the (101) diffraction intensity.

The composite MWNTs/PVA nanofibers not only showed a stronger (101) reflection, but also had a medium intensity (201) peak at 2θ =27^{o} (**Figure 5b**). The post-spinning treatments also influenced the diffraction patterns. Similar to the neat PVA nanofibers, the methanol treatment resulted in a greater (101) peak, and the emergence of (001) and (002) peaks. However, the crosslinking reaction did not reduce the (101) reflection much, which is quite different to the neat PVA nanofibers.

3.4. Mechanical properties

Tensile strength and strain values of both the neat PVA and the MWNTs/PVA composite nanofiber mats are listed in **Table 1**. The tensile strength and strain of the neat PVA nanofiber mat were 7.3MPa and 141%, respectively. The methanol treatment doubled the tensile strength of the nanofiber mat, but slightly decreased its strain at break. The crosslinking

treatment also increased the tensile strength of the nanofiber mat, but resulted in a lower strain value than the methanol treatment.

All composite nanofibers have higher tensile strength than their PVA nanofiber counterparts. Without any post-spinning treatment, the tensile strength of the MWNTs/PVA nanofiber mat was 4.24MPa, about 36.3% higher than that of the neat PVA counterpart. The post-spinning treatments improved the tensile strength. The methanol treatment led to 2.54 times increase in the tensile strength, and the crosslinking treatment doubled the tensile strength value. The nanofiber mat treated by both methanol and the crosslinking reaction showed the highest improvement in the tensile strength, 12.9MPa about 3.04 times higher than the un-treated composite nanofiber mat.

The tensile strength of electrospun nanofiber mat is associated with material properties, fiber morphology and web structure. As a result of random fiber collection and electrospinning under the same operating condition, the non-woven nanofiber mats have a similar web structure. To some extent, the tensile strength of the nanofiber mat reflects the strength of the constituent nanofibers. From neat PVA to MWNTs/PVA composite and to the post-treatments by methanol and crosslinking reaction, the material tensile strength was improved by 415% in total.

All the post-spinning treatments decreased the strain value. The crosslinked nanofiber mats had a lower strain value than those treated by methanol, because a crosslinked polymer network typically has greater restriction to mechanical deformation.

3.5. Water contact angle

The water contact angles of the PVA and the composite MWNTs/PVA nanofiber mats were listed in **Table 1**. PVA is hydrophilic in general, and the water droplet was adsorbed by the neat PVA nanofiber mat very quickly. The post-spinning treatments led to an increase in water contact angle. By comparison to un-treated nanofiber mat, the nanofiber mat treated by methanol had 40 degrees higher contact angle, while the crosslinked nanofiber mat had higher contact angle value than that treated by methanol, because the –OH groups in PVA are converted to acetal groups or ether linkages after crosslinking with glutaric dialdehyde[50].

The composite MWNTs/PVA nanofiber mat had about 30 degrees higher contact angle than the neat PVA nanofibers, and the post-spinning treatments resulted in further increase in the contact angle value. The lowered surface hydrophility resulting from the presence of carbon nanotubes in the PVA matrix suggested that the nucleation crystallization could influence the surface PVA morphology of the composite nanofibers.

As with the electrospinning of a polymer solution containing nano-sized fillers, the nano fillers are normally restricted within the inner side of the electrospun nanofibers, leaving a plain polymer shell on the surface[14, 15, 21, 22, 54]. The difference in the contact angle between the neat PVA and the MWNTs/PVA composite nanofiber mats should come from the effect of carbon nanotube on the PVA crystallinity and fiber surface morphology. **Figure 6** shows the correlation between the water contact angle and the crystallinity of PVA. Ignoring the presence of carbon nanotube and methanol treatment, a linear dependency between the PVA crystallinity and the water contact angle was obtained for the non-crosslinked nanofiber samples. It indicated that a higher PVA crystallinity resulted in higher contact angle value.

This can be attributed to the fact that the PVA in crystal is more difficult to be dissolved in water than its amorphous state because of stronger intermolecular hydrogen bonds among the PVA molecules in the crystal state [52]. A linear dependency between the PVA crystallinity and the water contact angle was also found for the crosslinked nanofibers, except that the crosslinked nanofibers showed a higher contact angle value.

It was also noticed that the crosslinked composite MWNTs/PVA nanofibers showed a higher contact angle than the un-treated one, even if they had similar PVA crystallinity content. This indicated that the crosslinking reaction took place on the surface of the composite nanofibers, but did not change the crystallinity characteristic of the whole nanofibers because of the presence of carbon nanotubes.

3.6. Thermal stability

The thermogravimetric curves give a direct view of polymer thermal degradation. As shown in **Figure 7a**, the neat PVA nanofibers started to lose weight at about 215^{o}C, with two main weight loss derivative peaks (DTG) at 243^{o}C and 442^{o}C. The post-spinning treatments increased the onset decomposing temperature (T_d) and shifted the DTG peaks. As listed in **Table 2**, the methanol treatment shifted T_d temperature to 269^{o}C, about 54^{o}C higher than that of the untreated PVA nanofibers. Also, the DTG peaks were shifted to a higher temperature. Similar to the methanol treatment, the crosslinking reaction shifted the T_d and DTG peaks to higher temperatures also.

The introduction of MWNTs in PVA resulted in different thermal degradation process. By comparison with the neat PVA counterpart, the un-treated MWNTs/PVA nanofibers have a

lower onset decomposing temperature (201^{o}C), and the 2nd DGA peak was decreased considerably (**Figure 7b**). The T_d and DTG peaks of the MWNTs/PVA nanofibers are also listed in **Table 2**. For the un-treated composite nanofibers, the 1st and 2nd DTG peak temperatures were at 286^{o}C and 441^{o}C, respectively. All the post-spinning treatments increased the T_d to about 260^{o}C, and shifted the 1st DTG peak to about 360^{o}C, while the 2nd DTG peak remained almost unchanged. The thermal degradation characteristics among the post-treated MWNTs/PVA nanofibers were quite similar to each other. The presence of carbon nanotube could stabilize the thermal degradation for the post-treated composite nanofibers.

4. Conclusions

This study has confirmed that the nucleation crystallization of PVA by carbon nanotubes also happens in electrospun CNTs/PVA composite nanofibers. This nucleation crystallization process is more likely to take place prior to electrospinning owing to the rapid fiber stretching and solidification process during electrospinning provides very limited time for the PVA to crystallize around the carbon nanotube. The increase in the crystallinity due to the presence of carbon nanotubes has considerably improved the tensile strength, but slightly reduced the strain at break of the CNTs/PVA nanofiber mats. The fiber tensile strength can be further improved through increasing the PVA crystallinity or the formation of crosslinked PAV network via soaking in methanol and a crosslink reaction, respectively. However, the presence of carbon nanotubes reduces the crystallization rate in the methanol treatment, but prevents the crystallinity reduction during the crosslinking reaction. With the increase in the PVA crystallinity, fiber tensile strength was further increased, but the surface hydrophilicity

reduced. In comparison to the crosslinking reaction, the methanol treatment resulted in better improvement in the fiber tensile strength and less reduction in the strain value.

These results suggest that the tensile strength and the surface hydrophobicity of CNTs/PVA composite fibers can be improved by a post-spinning treatment to increase the crystallinity of the PVA matrix or by establishing a crosslinked PVA network. A polymer that is able to form nucleation crystallization around carbon nanotubes should be a better choice to develop CNT composite nanofibers because of the enhanced interaction between carbon nanotube and the polymer matrix. Combining the nucleation crystallization of polymer matrix and post-treatments to improve matrix crystallinity will form an effective approach for developing high strength CNT composite materials.

Acknowledgments: This work was carried out through an International Postgraduate Research Scholarship (IPRS) awarded to the first author. The work was also supported by Deakin University under its Central Research Grant scheme.

References

[1] Ajayan, P M 1999 *Chemical Reviews* **99** 1787-1799
[2] Cadek, M, Coleman J N, Barron V, Hedicke Kand Blau W J 2002 *Applied Physics Letters* **81** 5123-5125
[3] Dalton, A B, Collins S, Munoz E, Razal J M, Ebron V H, Ferraris J P, Coleman J N, Kim B Gand Baughman R H 2003 *Nature* **423** 703
[4] Kilbride, B E, Coleman J N, Fraysse J, Fournet P, Cadek M, Drury A, Hutzler S, Roth Sand Blau W J 2002 *Journal of Applied Physics* **92** 4024-4030
[5] Sandler, J K W, Kirk J E, Kinloch I A, Shaffer M S Pand Windle A H 2003 *Polymer* **44** 5893-5899
[6] Biercuk, M J, Liaguno M C, Radosavljevic M, Hyun J K, Fischer J Eand Johnson A T 2002 *Applied Physics Letters* **80** 2767-2769
[7] Wei, C, Srivastava Dand Cho K 2002 *Nano Letters* **2** 647-650

[8] Vigolo, B, Penicaud A, Coulon C, Sauder C, Pailler R, Journet C, Bernier Pand Poulin P 2000 *Science* **290** 1331-1334
[9] Poulin, P, Vigolo Band Launois P 2002 *Carbon* **40** 1741-1749
[10] Munoz, E, Dalton A B, Collins S, Kozlov M, Razal J, Coleman J N, Kim B G, Ebron V H, Selvidge M, Ferraris J Pand Baughman R H 2004 *Advanced Engineering Materials* **6** 801-804
[11] Dalton, A B, Collins S, Razal J, Munoz E, Ebron V H, Kim B G, Coleman J N, Ferraris J Pand Baughman R H 2004 *Journal of Materials Chemistry* **14** 1-3
[12] Zhang, X, Liu T, Sreekumar T V, Kumar S, Hu Xand Smith K 2004 *Polymer* **45** 8801-8807
[13] Kozlov, M E, Capps R C, Sampson W M, Ebron V H, Ferraris J Pand Baughman R H 2005 *Advanced Materials* **17** 614-617
[14] Ko, F, Gogotsi Y, Ali A, Naguib N, Ye H, Yang G, Li Cand Wilis P 2003 *Advanced Materials* **15** 1161-1165
[15] Dror, Y, Salalha W, Khalfin R L, Cohen Y, Yarin A Land Zussman E 2003 *Langmuir* **19** 7012-7020
[16] Reneker, D H and Chun I 1996 *Nanotechnology* **7** 216-223
[17] Theron, S A, Zussman Eand Yarin A L 2004 *Polymer* **45** 2017-2030
[18] Li, D and Xia Y 2004 *Advanced Materials* **16** 1151-1170
[19] Subbiah, T, Bhat G S, Tock R W, Parameswaran Sand Ramkumar S S 2005 *Journal of Applied Polymer Science* **96** 557-569
[20] Shin, Y M, Hohman M M, Brenner M Pand Rutledge G C 2001 *Applied Physics Letters* **78** 1149-1151
[21] Gao, J, Yu A, Itkis M E, Bekyarova E, Zhao B, Niyogi Sand Haddon R C 2004 *Journal of the American Chemical Society* **126** 16698-16699
[22] Salalha, W, Dror Y, Khalfin R L, Cohen Y, Yarin A Land Zussman E 2004 *Langmuir* **20** 9852-9855
[23] Zhou, W, Wu Y, Wei F, Luo Gand Qian W 2005 *Polymer* **46** 12689-12695
[24] Ge, J J, Hou H, Li Q, Graham M J, Greiner A, Reneker D H, Harris F Wand Cheng S Z D 2004 *Journal of the American Chemical Society* **126** 15754-15761
[25] Hou, H, Ge J J, Zeng J, Li Q, Reneker D H, Greiner Aand Cheng S Z D 2005 *Chemistry of Materials* **17** 967-973
[26] Kim, G M, Michler G Hand Poetschke P 2005 *Polymer* **46** 7346-7351
[27] Jeong, J S, Jeon S Y, Lee T Y, Park J H, Shin J H, Alegaonkar P S, Berdinsky A Sand Yoo J B 2006 *Diamond and Related Materials* **15** 1839-1843
[28] Sundaray, B, Subramanian V, Natarajan T Sand Krishnamurthy K 2006 *Applied Physics Letters* **88** 143114/1-143114/3
[29] Wang, G, Tan Z, Liu X, Chawda S, Koo J-S, Samuilov Vand Dudley M 2006 *Nanotechnology* **17** 5829-5835
[30] Zhang, X, Liu T, Sreekumar T V, Kumar S, Moore V C, Hauge R Hand Smalley R E 2003 *Nano Letters* **3** 1285-1288
[31] Cadek, M, Coleman J N, Ryan K P, Nicolosi V, Bister G, Fonseca A, Nagy J B, Szostak K, Beguin Fand Blau W J 2004 *Nano Letters* **4** 353-356
[32] Coleman, J N, Blau W J, Dalton A B, Munoz E, Collins S, Kim B G, Razal J, Selvidge M, Vieiro Gand Baughman R H 2003 *Applied Physics Letters* **82** 1682-1684
[33] Probst, O, Moore E M, Resasco D Eand Grady B P 2004 *Polymer* **45** 4437-4443
[34] Chen, W, Tao X, Xue Pand Cheng X 2005 *Applied Surface Science* **252** 1404-1409

[35] Ryan, K P, Cadek M, Drury A, Ruether M, Blau W Jand Coleman J N 2005 *Fullerenes, Nanotubes, and Carbon Nanostructures* **13** 431-434
[36] Ciambelli, P, Sarno M, Gorrasi G, Sannino D, Tortora Mand Vittoria V 2005 *Journal of Macromolecular Science, Part B: Physics* **44** 779-795
[37] Minus, M L, Chae H Gand Kumar S 2006 *Polymer* **47** 3705-3710
[38] Bin, Y, Mine M, Koganemaru A, Jiang Xand Matsuo M 2006 *Polymer* **47** 1308-1317
[39] Koski, A, Yim Kand Shivkumar S 2003 *Materials Letters* **58** 493-497
[40] Lee, J S, Choi K H, Ghim H D, Kim S S, Chun D H, Kim H Yand Lyoo W S 2004 *Journal of Applied Polymer Science* **93** 1638-1646
[41] Zhang, C, Yuan X, Wu L, Han Yand Sheng J 2005 *European Polymer Journal* **41** 423-432
[42] Son, W K, Youk J H, Lee T Sand Park W H 2005 *Materials Letters* **59** 1571-1575
[43] Yao, L, Haas T W, Guiseppi-Elie A, Bowlin G L, Simpson D Gand Wnek G E 2003 *Chemistry of Materials* **15** 1860-1864
[44] Lin, T, Fang J, Wang H, Cheng Tand Wang X 2006 *Nanotechnology* **17** 3718-3723
[45] Zeng, J, Aigner A, Czubayko F, Kissel T, Wendorff J Hand Greiner A 2005 *Biomacromolecules* **6** 1484-1488
[46] Taepaiboon, P, Rungsardthong Uand Supaphol P 2006 *Nanotechnology* **17** 2317-2329
[47] Wang, X, Chen X, Yoon K, Fang D, Hsiao B Sand Chu B 2005 *Environmental Science and Technology* **39** 7684-7691
[48] Krimm, S, Liang C Yand Sutherland G B B M 1956 *Journal of Polymer Science* **22** 227-47
[49] Yeom, C-K and Lee K-H 1996 *Journal of Membrane Science* **109** 257-265
[50] Hyder, M N, Huang T Y Mand Chen P 2006 *Journal of Membrane Science* **283** 281-290
[51] Park, J-S, Park J-Wand Ruckenstein E 2001 *Journal of Applied Polymer Science* **82** 1816-1823
[52] Assender, H E and Windle A H 1998 *Polymer* **39** 4295-4302
[53] Nishio, Y and Manley R S 1998 *Macromolecules* **21** 1270-1277
[54] Liu, J, Wang T, Uchida Tand Kumar S 2005 *Journal of Applied Polymer Science* **96** 1992

Figure and Table captions

Figure 1: SEM images of the MWNTs/PVA nanofibers, (a) without treatment, (b) treated by methanol, (c) treated by crosslinking, (d) treated by methanol/crosslinking.

Figure 2: TEM image of the MWNTs/PVA nanofibers treated by methanol/crosslinking.

Figure 3: FTIR spectra of the MWNTs/PVA nanofibers before and after crosslinking reaction.

Figure 4: DSC curves of (a) neat PVA nanofibers, and (b) MWNTs/PVA (4.5 wt %) nanofibers

Figure 5: Wide Angle X-rag diffraction (a) neat PVA nanofibers and (b) MWNTs/PVA nanofibers.

Figure 6: Water contact angle versus crystallinity. The linear fitting for the non-crosslinked nanofiber samples is $\alpha = -176.3 + 6.1\chi$ (Correlation coefficient, R=0.96); while for the crosslinked nanofiber samples is $\alpha = -5.0 + 2.8\chi$ (R=0.92).

Figure 7: TGA curves of (a) neat PVA nanofibers, and (b) MWNTs/PVA nanofibers

Table 1: Fiber diameters, tensile properties and water contact angles

Table 2: Melting point, crystallinity content and thermal degradation data

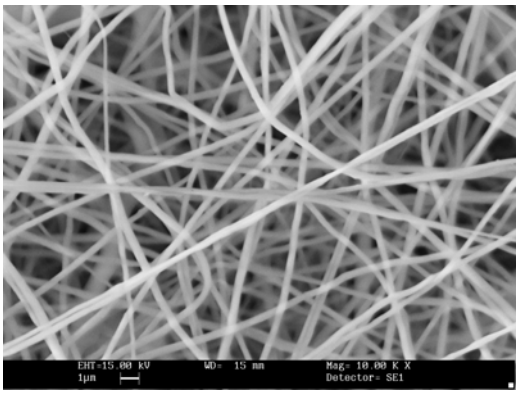

(a)

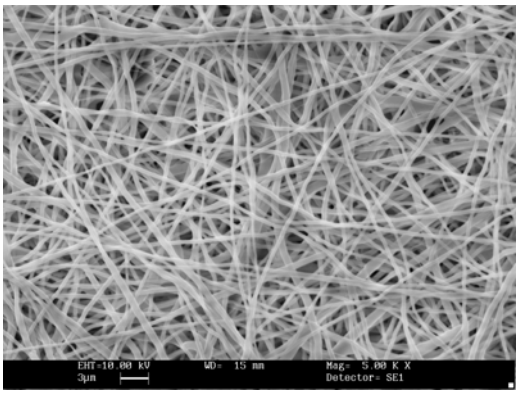

(b)

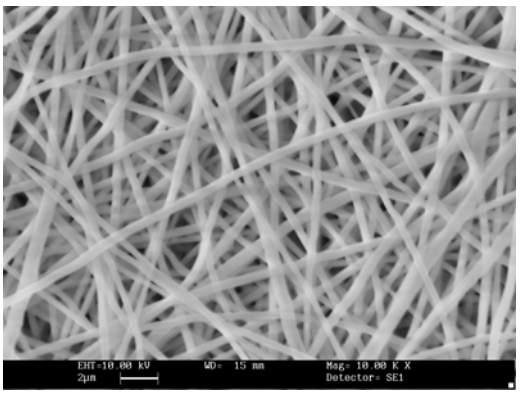

(c)

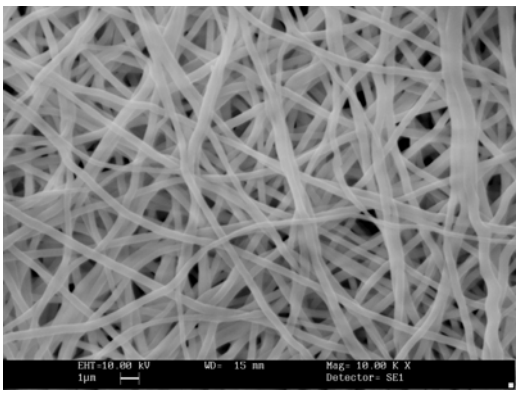

(d)

Figure 1: SEM images of the MWNTs/PVA nanofibers, (a) without treatment, (b) treated by methanol, (c) treated by crosslinking, (d) treated by methanol/crosslinking.

Figure 2: TEM image of the MWNTs/PVA nanofibers treated by methanol/crosslinking.

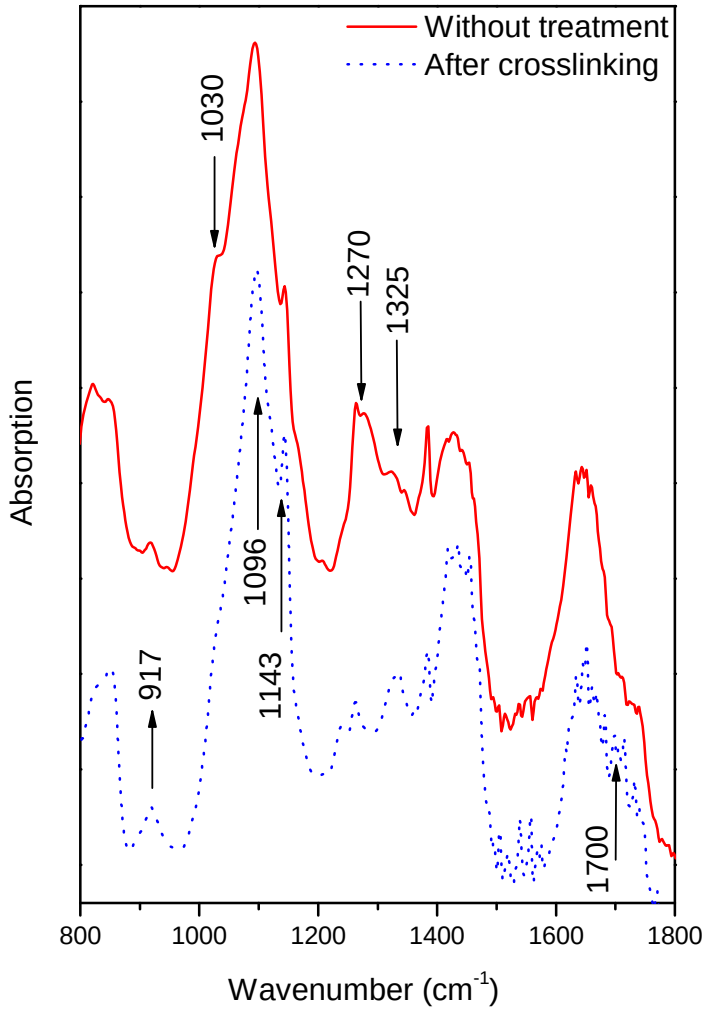

Figure 3: FTIR spectra of the MWNTs/PVA nanofibers before and after crosslinking reaction.

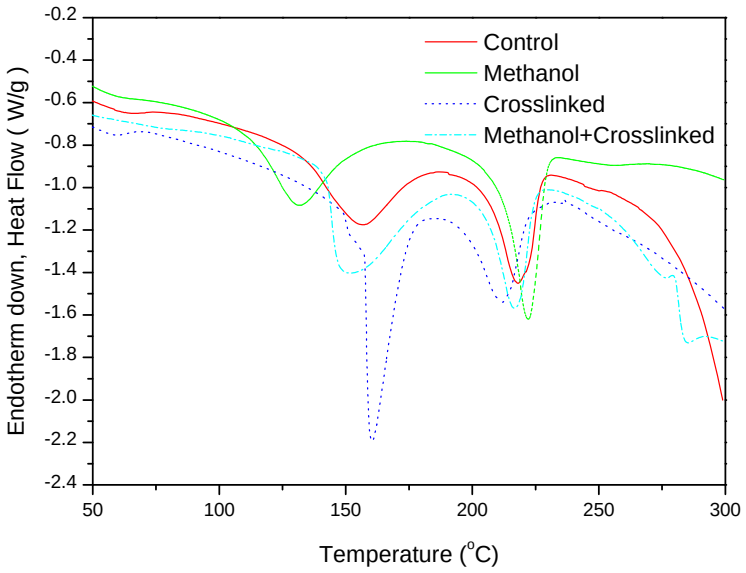

(a)

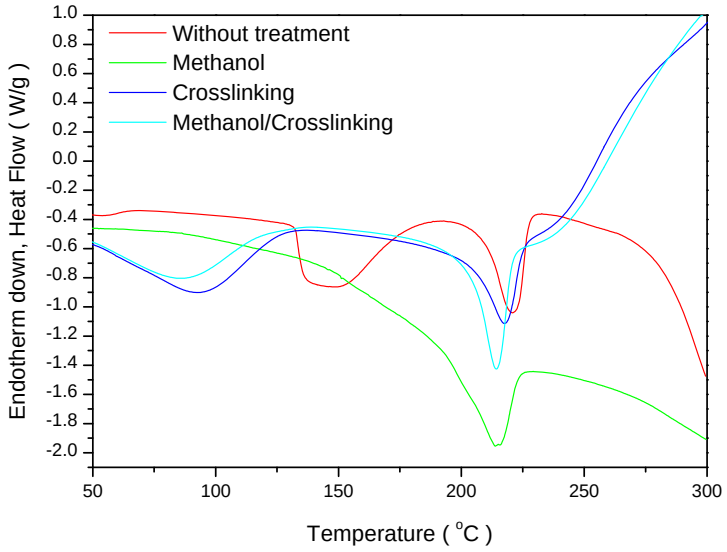

(b)

Figure 4: DSC curves of (a) neat PVA nanofibers, and (b) MWNTs/PVA (4.5 wt %) nanofibers

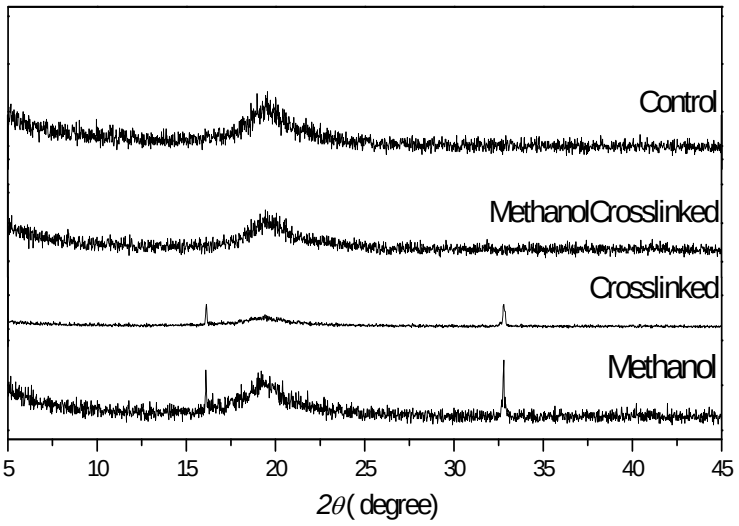

(a)

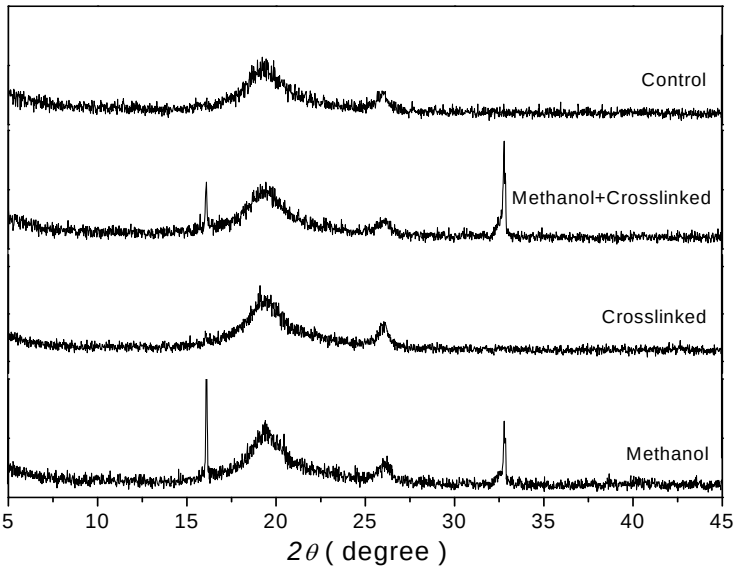

(b)

Figure 5: Wide Angle X-rag diffraction (a) neat PVA nanofibers, and (b) MWNTs/PVA nanofibers.

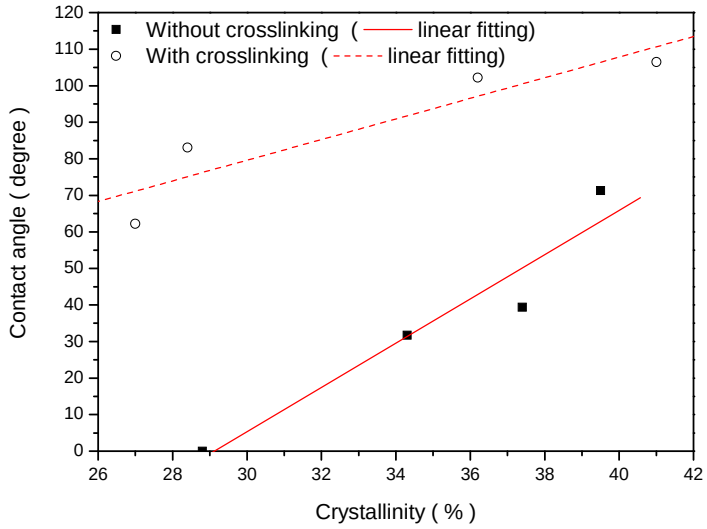

Figure 6: Water contact angle versus crystallinity. The linear fitting for the non-crosslinked nanofiber samples is $\alpha = -176.3 + 6.1\chi$ (Correlation coefficient, R=0.96); while for the crosslinked nanofiber samples is $\alpha = -5.0 + 2.8\chi$ (R=0.92).

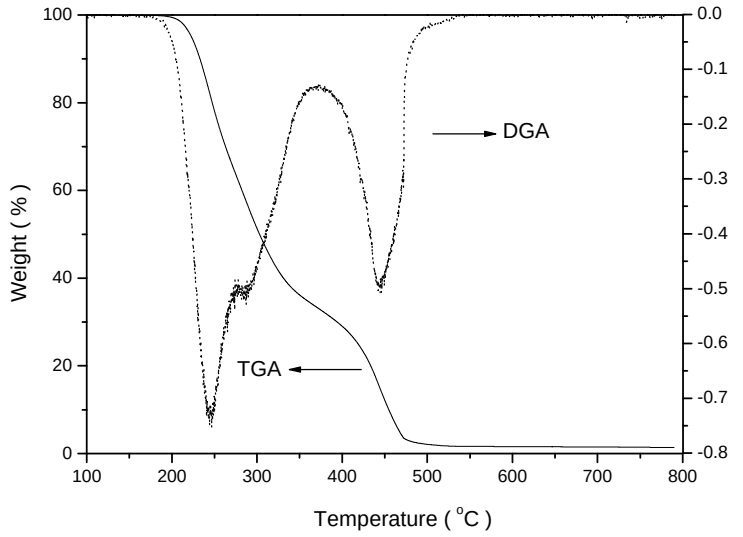

(a)

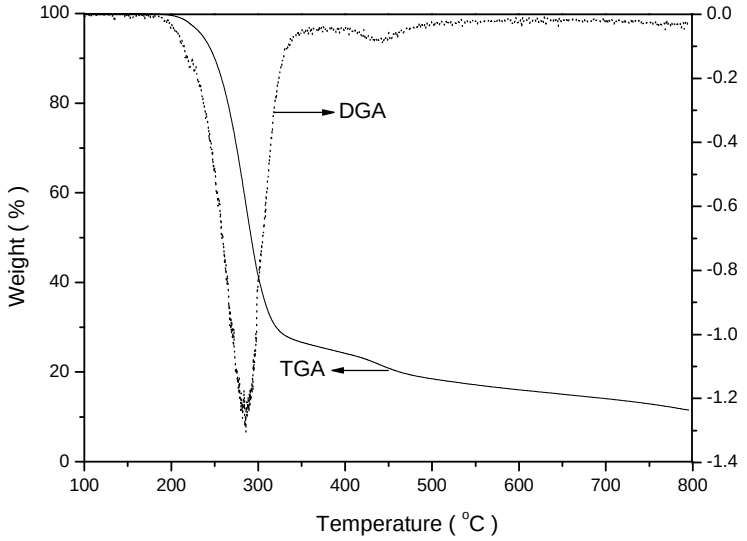

(b)

Figure 7: TGA curves of (a) neat PVA nanofibers, and (b) MWNTs/PVA nanofibers

Table 1: Fiber diameters, tensile properties and water contact angles

	Pure PVA Nanofiber Mats				MWNTs/PVA Nanofiber Mats			
	Diameter (nm)	Tensile strength (MPa)	Strain (%)	Contact Angle	Diameter (nm)	Tensile strength (MPa)	Strain (%)	Contact Angle
Non-treatment	684±220	3.11	141.72	-	295±4	4.24	142.54	31.7
Methanol	673±183	7.32	138.04	39.4	393±11	10.78	132.18	71.3
Crosslinking	700±224	6.05	90.59	62.2	429±8	8.48	104.53	102.2
Methanol/Crosslink	630±179	8.33	102.64	83.1	382±12	12.9	96.3	106.5

Table 2: Melting point, crystallinity content and thermal degradation data

	Pure PVA Nanofibers						MWNTs/PVA Nanofibers					
	T_m (^oC)	ΔH (J/g)	χ (%)	Onset (^oC)	1st Peak	2nd Peak	T_m (^oC)	ΔH (J/g)	χ (%)	Onset (^oC)	1st Peak	2nd Peak
Non-treatment	218.0	44.6	28.8	215	243	442	221.1	53.2	34.3	201	286	441
Methanol	222.2	57.9	37.4	269	369	575	213.8	61.3	39.5	262	365	442
Crosslinking	211.5	41.8	27.0	245	294	510	217.9	56.1	36.2	258	359	430
Methanol/Crosslink	216.8	44.0	28.4	253	310	522	214.1	62.2	40.1	261	357	424